# Critical suction pressure during installation of suction caissons in sand

Panagoulias, S.; van Dijk, B.F.J.; Drummen, T.; Askarinejad, Amin; Pisano, F.

**DOI**
10.3723/osig17.570

**Publication date**
2017

**Document Version**
Final published version

**Published in**
Proceedings of the 8th Offshore Site Investigation and Geotechnics International Conference, 12-14 September 2017

**Citation (APA)**
Panagoulias, S., van Dijk, B. F. J., Drummen, T., Askarinejad, A., & Pisano, F. (2017). Critical suction pressure during installation of suction caissons in sand. In *Proceedings of the 8th Offshore Site Investigation and Geotechnics International Conference, 12-14 September 2017: Offshore site investigation and geotechnics. Smarter Solutions for Future Offshore Developments London, UK* (pp. 570-577) https://doi.org/10.3723/osig17.570

# CRITICAL SUCTION PRESSURE DURING INSTALLATION OF SUCTION CAISSONS IN SAND

S Panagoulias
*Plaxis, Delft (formerly Fugro, Nootdorp), The Netherlands*

BFJ van Dijk and T Drummen
*Fugro, Nootdorp, The Netherlands*

A Askarinejad and F Pisanò
*Delft University of Technology, Delft, The Netherlands*

**Abstract**
When installing suction caissons in sand, the suction process will induce an upward flow, which reduces the effective stress in the soil inside the caisson. The suction pressure cannot be increased indefinitely. If a critical suction pressure is exceeded, liquefaction, boiling and/or piping occurs. This will halt the installation process. This paper presents results from a novel laboratory upward flow test (LUFT), to investigate the soil mechanisms affecting the critical suction pressure. The LUFT apparatus is based on a conventional permeameter. As suggested by the results of published full/small scale installation tests, LUFT results confirm that, in dense to very dense sand, most conventional critical suction prediction models underestimate the values observed in reality. It is argued that soil arching contributes to the achievable high values for critical suction pressure. Higher allowable suction pressures may be cost effective.

## 1. Introduction

Suction caissons have been deployed in the last three decades in a growing number of offshore developments, for bottom-fixed and floating structures, in shallow and deep waters (Tjelta, 2015). The number of suction caisson installations in sand is much lower than in clay.

When installing suction caissons (also referred to as suction piles or suction buckets) in sand, the suction pressure is limited by a critical value. At the critical suction pressure liquefaction, boiling and/or piping will occur, which may lead to excessive plug heave and may halt the installation process.

The literature about successful installations of suction caissons in sand indicates that in quite a few cases suction pressures have been applied above the level predicted by conventional critical suction pressure models. If a higher critical suction pressure can be relied upon, then the length of the skirts may be increased and thus the capacity for the same diameter. Indeed increasing the skirt length is more cost effective than increasing the diameter. It is noted that for higher suction pressures there is potential for loosening the soil inside and below the caisson, which may lead to a reduction in capacity. However, experiences from several prototype and model test suction caisson installations have shown that gradients close to critical can be applied without significant detrimental consequences (Andersen et al., 2008). In this article, the results of simple upward flow laboratory tests are discussed to gain qualitative insight into the possible factors that enhance the resistance of the sand plug to piping/liquefaction during suction installation.

## 2. Field Observations

Conventional design approaches define the critical suction pressure as the pressure for which the effective vertical stress in the sand reduces to zero inside the caisson. This is often related to the critical (exit) hydraulic gradient $i_{cr,th}$ (-) (Senders and Randolph, 2009) and the effective unit weight γ' (kN/m$^3$) of the soil:

$$i_{cr,th} = \frac{\gamma'}{\gamma_w} \qquad (1)$$

where $\gamma_w$ = unit weight of water (kN/m$^3$).

Different models to assess the critical suction pressure in sand have been proposed, such as described by Erbrich and Tjelta (1999), Feld (2001), Houlsby and Byrne (2005), Senders and Randolph (2009) and Ibsen and Thilsted (2010). Houlsby and Byrne (2005) describe a theoretical model to assess the critical suction pressure, where they considered a change in the permeability inside the suction caisson by a ratio of $k_r = k_i/k_o$ (-), due to a reduction in effective stress, where $k_i$ (m/s) is the permeability of the soil inside the caisson and $k_o$ (m/s) is the permeability of the soil outside the caisson. The Erbrich and Tjelta (1999) method and Houlsby and Byrne (2005) method for kr = 1 and for kr = 3 encompass all the other models. The Houlsby and Byrne (2005) method for kr = 1 and for kr = 3 has been compared with suction caisson installation data from six locations in the North Sea (Table 1), all involving silica/quartz sands.

*Table 1: Suction installation data from six locations in the North Sea*

| Project | L (m) | D (m) | $D_r$ | Reference |
|---|---|---|---|---|
| Europipe field test | 1.65 | 1.5 | Very dense | Senders and Randolph (2009) |
| Tenby | 1.4 | 2.0 | Dense | Houlsby and Byrne (2005) |
| Calder | 5.75 | 9.25 | Very loose to very dense | Heuvel and Riemers (2005) |
| Luce bay | 1.0<br>1.5 | 1.5<br>3.0 | Dense | Houlsby et al. (2006) |
| Jacky B12/21 | 7.0 | 10.0 | Dense to very dense | Chatzivasileiou (2014) |
| L6-B | 10.0 | 10.0 | Very loose to very dense | Alderlieste and Van Blaaderen (2015) |

where $L$ = skirt length, $D$ = caisson diameter and $D_r$ = relative density.

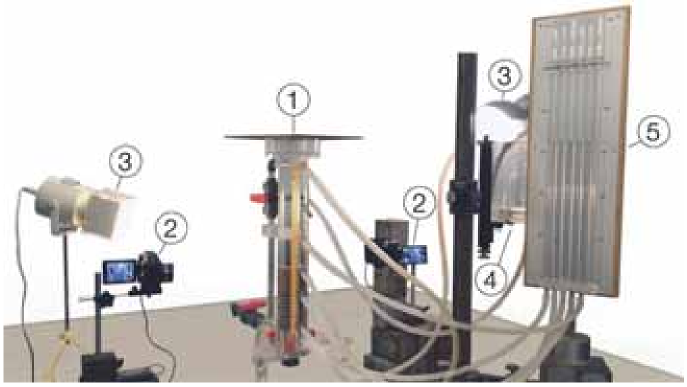

Figure 2: LUFT test set-up – (1) permeameter, (2) side cameras, (3) light source, (4) inflow tank, (5) standpipe board

The penetration curves in Figure 1 show that in most cases the applied suction pressure was above the theoretical critical suction pressure predicted according to Houlsby and Byrne (2005), for $k_r = 3$. No adverse effects, such as excessive heave, were reported in any of the cases considered – in agreement with the above mentioned observations by Andersen et al. (2008).

### 3. LUFT model

To gain more insight into the suction installation process, LUFTs were carried out (Panagoulias, 2015). The experimental set-up is presented in Figure 2. For the test a standard permeameter was used as described in ASTM (2006). The tests were performed under normal gravity (1g) conditions.

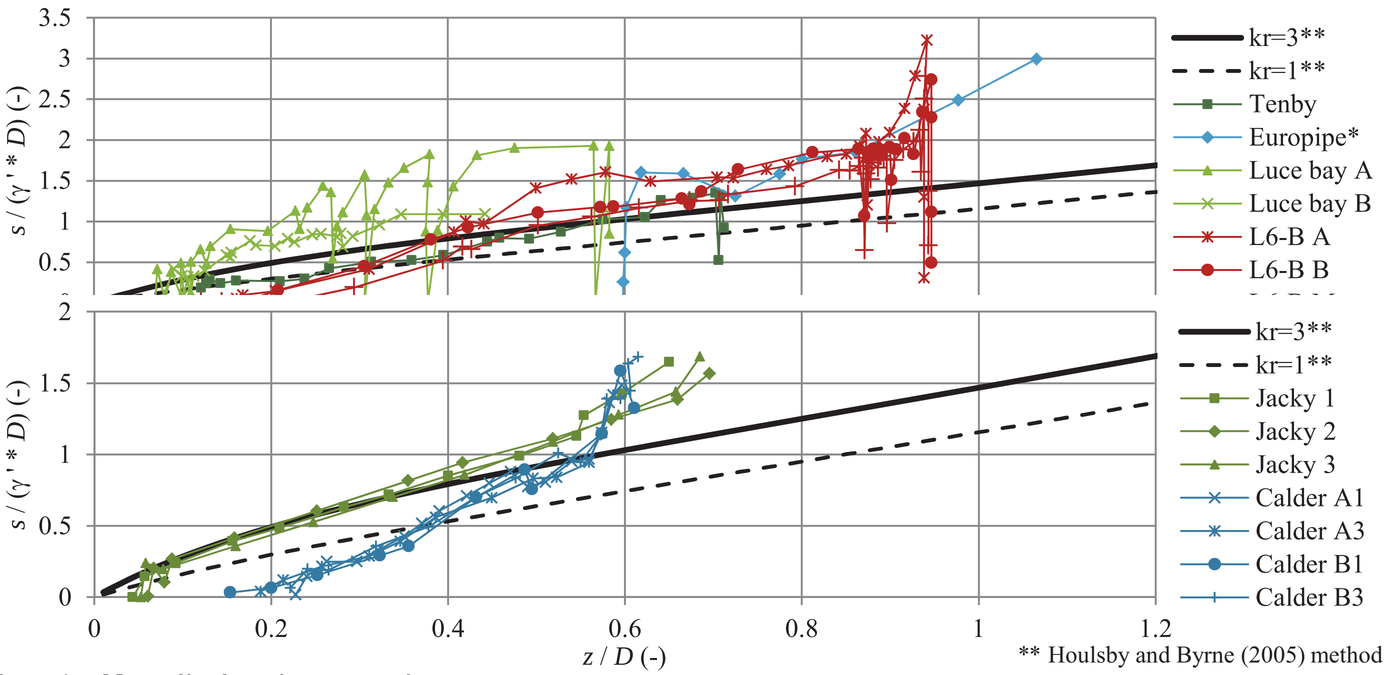

Figure 1: Normalised suction penetration curves.
Where s = applied suction (kPa), γ' = effective soil weight (kN/m3) and z = penetration depth (m)

The permeameter set-up was slightly modified to serve the purpose of the research (Figure 2):

- The permeameter was endowed with six piezometers.
- Vertical upward displacement of the soil was not prevented.
- Partially filled permeameter. Different specimen height $L_e$ (m) over diameter $D$ (m) ratios λ (-) were set by varying the height of the sand specimens (Figure 3).
- Metallic spheres were inserted beneath the sand specimens to ensure high permeability at the bottom, obtain uniform upward flow and have at least one piezometer measuring the pore pressure within the specimen (Figure 3).

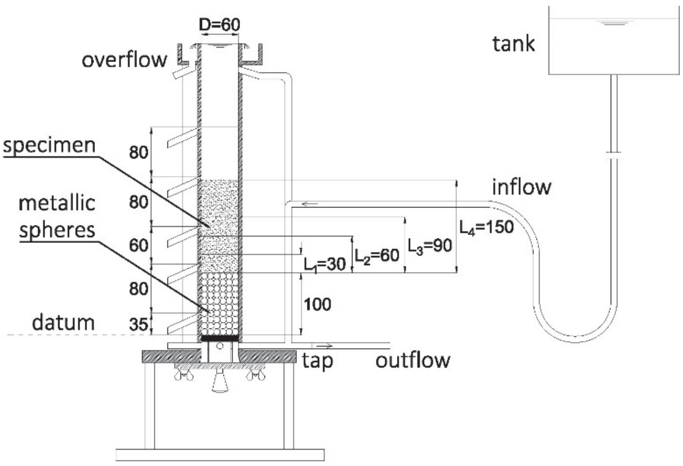


Figure 3: Schematisation of the LUFT with four different specimen heights ($L_1$, $L_2$, $L_3$ and $L_4$)

Two cameras were placed to capture images from opposite sides of the permeameter and allowed to quantify sand heave via particle image velocimetry (PIV) (White et al., 2003) analysis. The open-source, Matlab-based software PIVlab was used for PIV analyses (Thielicke & Stamhuis, 2014).

LUFT experiments target a simplified experimental simulation of prototype suction installation. These simple experiments focus on the interaction between soil plug and upward flow excluding factors that would bring in additional complexity, such as skirt skin friction and transient flow conditions. As outlined below, LUFT experiments are not exhaustive physical modelling of suction installation, but certainly help shed light on important factors affecting the achievement of critical suction conditions.

The prototype suction caisson installation process is a two-dimensional (2D) axisymmetric process with curved flowlines, whereas the LUFT experiment is a one-dimensional (1D) process with straight flowlines (Figure 4). The assumption of uniform flow pattern is valid for aspect ratios λ greater than 1.0, as the pore pressure difference across the tip level is less than 10% of the applied suction (Panagoulias, 2015). Different seepage conditions were tested in the LUFT apparatus by keeping the same soil configuration in each test, i.e. by producing a steady-state flow representation of different installation stages/scenarios. Although transient flow conditions arise during prototype installation, finite element method transient flow analyses indicated that the time needed to obtain steady-state flow conditions is small compared to the installation time and hence the flow conditions for a prototype installation are in fact close to steady-state (i.e. in the time needed to obtain steady state, the suction caisson will only have advanced a little further into the soil) (Panagoulias, 2015). Steady state conditions are also assumed in conventional suction caisson installation design.

LUFT experiments were performed using a Perspex permeameter. It should be noted that real prototypes feature steel skirts with a different interface friction than that of the Perspex permeameter.

### 4. Specimen characteristics and preparation

"Calibrated/filter sand" (fine grained with natural rounded particles, quartz percentage: 96%) and four different gradations were used (ASTM, 2011):

- specimen type S1, uniform, fine sand;
- specimen type S2, uniform, medium sand;
- specimen type S3, gap-graded, fine to medium sand, internally stable (Chang & Zhang, 2013); and
- specimen type S4, poorly graded, fine to medium sand.

The particle size distributions (PSDs) associated with each specimen type are presented in Figure 5 and further detailed in Table 2.

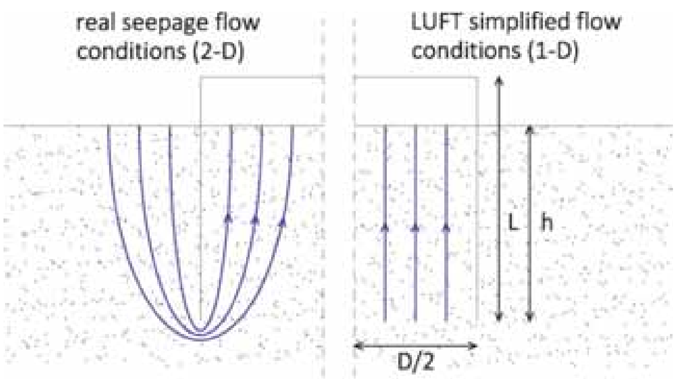


Figure 4: Flow conditions of prototype and LUFT

All specimens were prepared by combining wet pluviation and moist tamping, while ensuring full-saturation according to ASTM (2006) procedures. Prior to each experiment, a hydraulic steady- state condition in the specimen was achieved.

**5. Experimental programme and procedures**

Twenty-five LUFT experiments (Table 3) were performed to investigate the effects of:

- Sand relative density $D_r$ (-) – dense, medium dense and loose specimens have been tested.
- Specimen gradation – the four types as indicated in Table 2.
- Specimen aspect ratio λ – four different values: 0.5, 1.0, 1.5 and 2.5 (the last case was considered to confirm trends, even though installation of suction caissons with λ =2.5 is unlikely to be feasible in sand).

*Table 2: Specimen properties*

| Parameter | Unit | S1 | S2 | S3 | S4 |
|---|---|---|---|---|---|
| $d_{max}$ | mm | 0.21 | 0.50 | 0.50 | 0.50 |
| $d_{min}$ | mm | 0.15 | 0.42 | 0.15 | 0.13 |
| $d_{10}$ | mm | 0.16 | 0.43 | 0.18 | 0.15 |
| $d_{30}$ | mm | 0.17 | 0.45 | 0.33 | 0.25 |
| $d_{50}$ | mm | 0.18 | 0.46 | 0.39 | 0.36 |
| $d_{60}$ | mm | 0.19 | 0.47 | 0.43 | 0.43 |
| $Cu=d_{60}/d_{10}$ | - | 1.20 | 1.09 | 2.35 | 2.83 |
| $Cc=d_{30}^2/d_{10}d_{60}$ | - | 0.97 | 0.99 | 1.43 | 0.98 |
| $e_{min}$ | - | 0.60 | 0.56 | 0.51 | 0.50 |
| $e_{max}$ | - | 0.86 | 0.75 | 0.71 | 0.57 |
| $G_s$ | - | 2.64 | 2.65 | 2.64 | 2.64 |

where $d_{max}$ = maximum sand grain diameter, $d_{min}$ = minimum sand grain diameter, $d_n$ sand grain diameter at $n$% of the cumulative particle size distribution, $C_u$ = coefficient of uniformity, $C_c$ = coefficient of curvature, $e_{min}$ = minimum void ratio, $e_{max}$ = maximum void ratio and $G_s$ = specific gravity of solids.

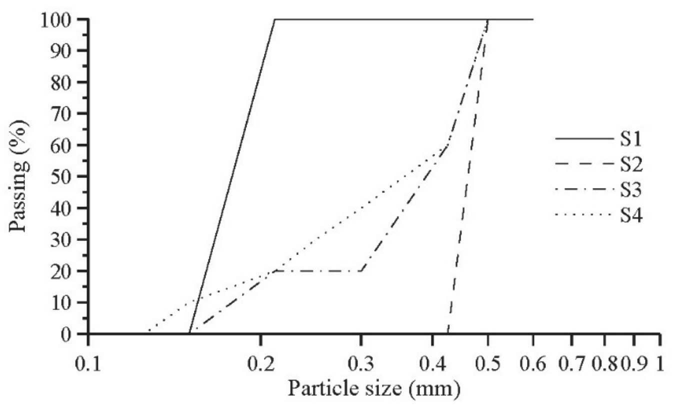


Figure 5: Particle size distributions of the specimen types

At the beginning of each LUFT experiment a low hydraulic gradient $i_{cr,e}$ (<0.1) was first enforced. Stepwise, the de-aired water level of the inflow tank was increased to the next desired hydraulic head difference $\Delta h$ (m), initially with step increments of 5 to 10 mm and then with smaller increments of 1-2 mm when approaching critical conditions. After reaching steady-state flow conditions, the hydraulic head $h$ (m) of each piezometer and the flow rate $q$ (m/s) were measured. Depending on the specimen height, one or more piezometers were used to calculate the global mean value of the hydraulic gradient along the specimen. Photos were also taken to enable PIV analysis.

The hydraulic head was step-wise increased until specimen instability, occurring in the form of global liquefaction, local piping or cracking. From this hydraulic head the critical difference in hydraulic head $\Delta h_{cr,e}$ (m) over the specimen and the average critical gradient $i_{cr,e} = \Delta h_{cr,e}/L_e$ (-) were calculated and compared with $i_{cr,th}$ as defined in Equation (1).

**6. Experimental results**

The results of the LUFT experiments are presented in Figures 6 and 7. As for the field data, the LUFT results indicate that the hydraulic gradient can be higher than the theoretical value (Equation 1). From the experiments the following trends were observed:

- for loose and medium dense specimens the $i_{cr,e}/i_{cr,th}$ ratio was around 1 (Figures 6b and 7b);
- for dense to very dense specimens the $i_{cr,e}/i_{cr,th}$ ratio increased up to 1.2 with increasing λ for non-uniform specimens (S3 and S4) (Figure 6a); and
- the uniformly graded specimens (S1 and S2; lower $C_u$) generally had a lower $i_{cr,e}/i_{cr,t\eta}$ ratio than the non-uniformly graded specimens (S3 and S4; higher $C_u$) (Figure 7a).

*Table 3: LUFT experimental programme*

| Experiment | λ | $D_r$ | Specimen type |
|---|---|---|---|
| 1 and 2 | 0.5 | Medium dense | S1 |
| 3 | 0.5 | Very dense | S1 |
| 4 | 1 | Loose | S1 |
| 5 and 6 | 1 | Very dense | S1 |
| 7 | 1.5 | Very loose | S1 |
| 8 | 1.5 | Very dense | S1 |
| 9 | 0.5 | Medium dense | S2 |
| 10 | 0.5 | Dense | S2 |
| 11 | 1 | Loose | S2 |
| 12 and 13 | 1 | Very dense | S2 |
| 14 and 15 | 1.5 | Very loose | S2 |
| 16 and 17 | 1.5 | Very dense | S2 |
| 18 | 2.5 | Very dense | S2 |
| 19 | 0.5 | Very dense | S3 |
| 20 | 1 | Medium dense | S3 |
| 21 | 1 | Very dense | S3 |
| 22 and 23 | 1.5 | Very dense | S3 |
| 24 | 2.5 | Very dense | S3 |
| 25 | 1 | Very dense | S4 |

### *6.1 Experimental uncertainty*

The inherent uncertainty of experimental measurements was estimated through an error propagation analysis based on the following assumptions:

- the absolute errors are normal (Gaussian) random variables;
- the variables are independent; and
- the variables are uncorrelated (i.e. covariance is zero).

The absolute uncertainties estimated for the main variables of the experiments are listed in Table 4. For each test the uncertainty is also represented by error bars in Figures 6 and 7.

*Table 4: Estimated uncertainties*

| Variable | Symbol | Uncertainty | Unit |
|---|---|---|---|
| Specimen diameter | $\delta D_{in}$ | ±0.04 | mm |
| Specimen height | $\delta L_e$ | ±0.2 | mm |
| Specimen degree of saturation | $\delta S_r$ | ±2.0 | % |
| Hydraulic head | $\delta h$ | ±0.5 | mm |
| Time | $\delta t$ | ±0.1 | s |

Note: For experiment 24 steady-state could not be reached at the end. This has resulted in a high assessed uncertainty for experiment 24 (Figures 6a and 7a).

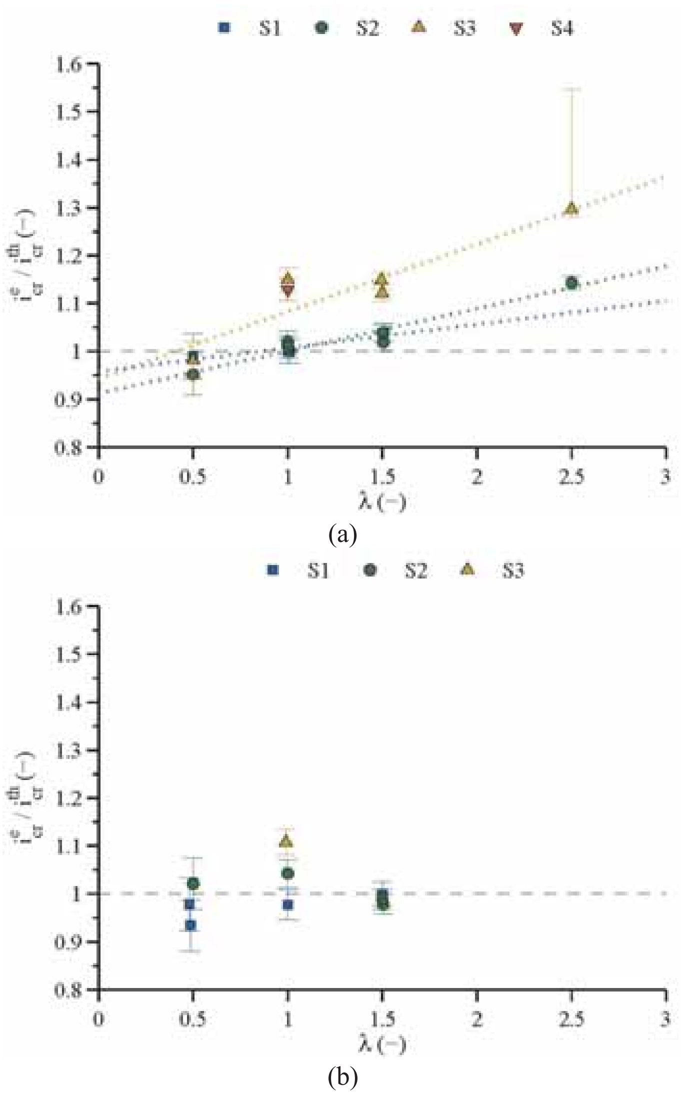


Figure 6: Results of the experiments including uncertainty range for (a) dense to very dense and (b) very loose to medium dense sand

### *6.2 Soil arching*

It was expected that soil arching would provide resistance to withstand a hydraulic gradient larger than the theoretical critical gradient in Equation 1.

Soil arching is the transfer of pressure from yielding soil masses onto adjoining stationary parts by shear resistance, reducing the pressure on the yielding part and increasing the pressure on the stationary part (Terzaghi, 1943). As for the skirts of the prototype, the wall of the permeameter is stiffer than the soil and hence the load arches onto the structure during the upward water flow, due to structure-soil interface friction (Villalobos, 2007). Friction and granular interlocking mechanisms enhance the vertical effective stresses in the soil, and in turn the critical suction pressure. These effects are expectedly magnified in denser specimens by the interaction between soil dilation and the lateral constraint imposed by the rigid permeameter wall.

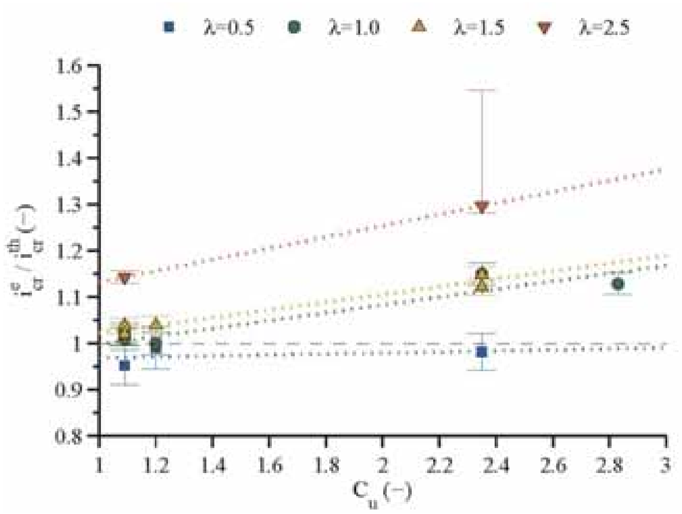


(a)

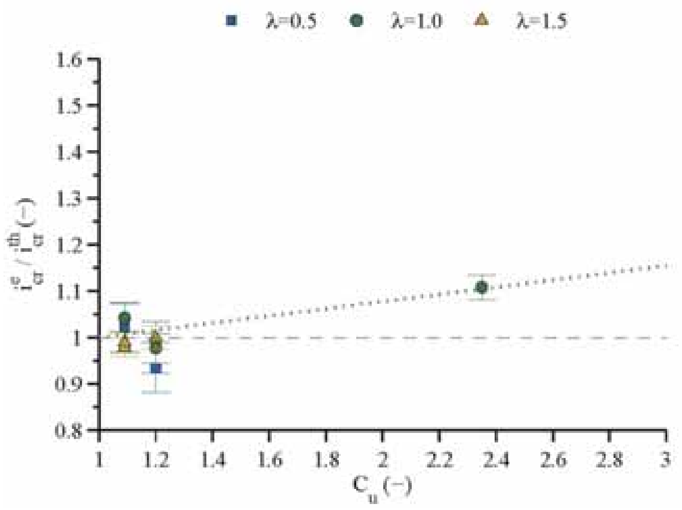


(b)

Figure 7: Results of the experiments including uncertainty range for (a) dense to very dense and (b) very loose to medium dense sand

The following phenomena observed during the experiments may be attributed to arching effects:

- The increasing trend of the $i_{cr,e}/i_{cr,th}$ ratio with respect to the relative density (Figure 6a and 6b). A higher relative density results in a higher initial horizontal $\sigma'_{h0}$ (kPa) to vertical $\sigma'_{v0}$ (kPa) effective stress ratio $K_0 = \sigma'_{h0}/\sigma'_{v0}$, a higher soil-wall interface friction, increased vertical effective stress and hence higher critical suction pressure.
- The increasing trend of the $i_{cr,e}/i_{cr,th}$ ratio with respect to λ for dense to very dense specimens (Figure 6a). An increase in specimen height provides more soil-wall interface friction.

As the interface friction of the prototype (soil-steel) is higher than the soil-Perspex interface in the LUFT, higher hydraulic gradients may be expected for offshore suction caissons.

These findings are also corroborated by the experimental results of Fleshman & Rice (2014), who performed upward flow tests in both uniform and graded sands by keeping λ=2.5. Fleshman & Rice reported $i_{cr,e}/i_{cr,th}$ ratios in the range from 1.15 to 2.4. These values, which are higher than found in the LUFT experiments, are likely to stem from the silicone gel used to enhance wall friction.

### *6.3 Specimen gradation*

A higher $i_{cr,e}/i_{cr,th}$ ratio for non-uniformly graded specimens was observed compared to specimens with a uniform particle size (Figure 7). Although the reason for this finding is not readily apparent, possible explanations may be:

- Uniformly graded specimens generate less wall friction compared to the non-uniformly graded specimens, as for the latter specimens the smaller particles fill in the voids between the larger particles and hence there is more particle contact.
- There is more particle contact within the non-uniformly graded specimens. The larger voids are filled with fine particles, and hence the granular structure of non-uniform specimens is expected to be stronger when compacted.
- Migration of fine particles into larger voids in the non-uniformly graded specimens. This affects the granular structure of the specimens, increasing the particle contact and making them possibly stronger or more stable.

### *6.4 Observed failure mechanisms*

Two types of failure mechanisms were observed during the LUFT experiments, piping and localised cracking (Figure 8).

Piping, occurred either inside the specimen or along the Perspex wall. The uniform specimens (S1 and S2) primarily failed by piping. In presence of sufficiently high hydraulic gradients, seepage forces displace sand particles until the formation of a preferential flow path (Figure 8a).

Localised cracking has been mainly observed in non-uniform specimens (S3 and S4) (Figure 8b). While increasing the hydraulic gradient, a horizontal crack occurred, lifting part of the specimen upwards. Possibly the arching mechanism prevented piping while the wall friction allowed the specimen to resist a hydraulic gradient higher than $i_{cr,th}$. In this case arching increased the resistance to piping and cracking, in a possibly less densified part of the specimen, was a weaker mechanism. It should be noted that localised cracking might be a typical feature of the LUFT, and in fact no field data are available to confirm that cracking might be a failure mechanism for the prototype.


(a) Piping


(b) Localised cracking

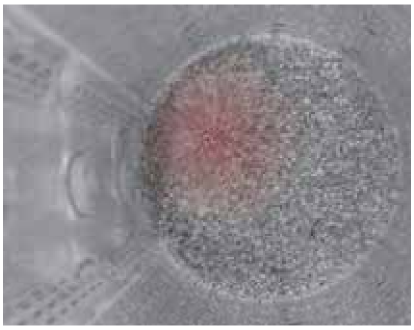
(c) Piping (top view)

Figure 8: Observed failure mechanisms

*6.5 Deformations*

The PIV analysis allowed to quantify specimen deformations, including heave. Results are plotted in Figure 9 as vertical strain ($\varepsilon_v = \Delta L/L_e$) against the coefficient of uniformity ($C_u$).

The mean $\varepsilon_v$ observed in the experiments, at the onset of failure, was approximately 1%, with maximum observed values of up to 3% in tests #12 and #13 (Table 3).

Lower vertical strain values have been observed for non-uniform specimens, possibly due to arching effects. The vertical strain, measured in the LUFT experiments was much lower than the heave ($h_s$) over installation depth ($L$) ratio of 8% to 10% for the centrifuge tests reported by Allersma et al. (1997) and the $h_s/L$ ratio of 4% to 20% measured in 1-g tests by Tran (2005). The experiments by Allersma et al. (1997) and Tran (2005) both involved actual penetration of a model caisson into sand, whereas that was not the case for the LUFT experiments.

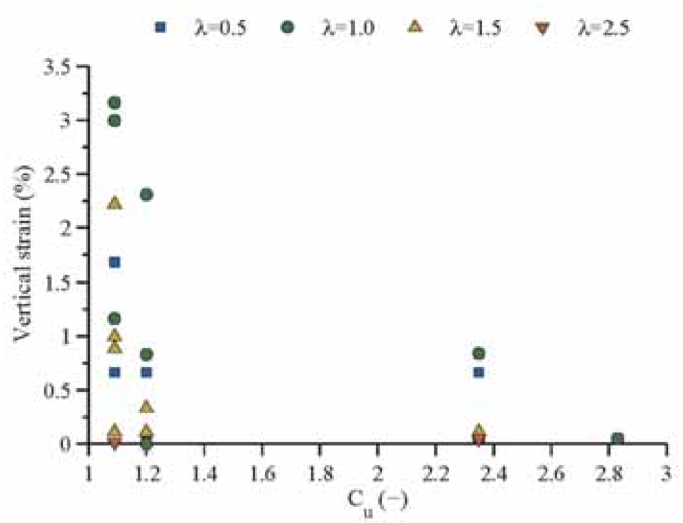


Figure 9: Vertical specimen strain at the onset of failure

Hence the observed differences might be (partially) due to:

- The volume of the skirt pushing the sand aside during installation, which due to the suction inside the caisson is assumed to mainly displace into the caisson interior. For the experiments by Allersma et al (1997) and Tran (2005) the wall thickness ($d$) to diameter ratio was between 0.5% to 2%. Since the $h_s/L$ ratio is approximately four times the $d/D$ ratio the $h_s/L$ ratio was between 2% and 8%.
- Displacement of sand from below the base of the caisson into the caisson interior due to suction.

**7. Concluding remarks**

Published suction caisson installation data indicate that hydraulic gradients higher than predicted by conventional models may be applied without inducing soil plug failure in the form of piping, boiling or excessive heave. The LUFT experiments support the expectation that this may be attributed to soil arching inside the suction caisson. The experiments also indicated that arching may not occur for:

- very loose to medium dense sand;
- possibly for small $L/D$ ratios; and
- possibly for uniform sand.

It is recommended, if arching is not expected to occur, not to exceed the hydraulic gradient assessed with conventional models such as Equation 1. For non-uniform dense to very dense sand, higher hydraulic gradients than assessed with conventional models can be achieved.

Although restricted to 1g-1D conditions, the LUFT investigation provides factual insight into which sand conditions have potential for increased critical suction pressure, and on the expected associated geotechnical mechanisms. In the authors' view, contributions kept on the descriptive side can impact the state of the art by warning on current practice, provision of possible optimisation opportunities and indicating the route for further investigations. In this case, centrifuge testing seems a future viable option to better quantify critical hydraulic gradient conditions.

**8. Acknowledgements**

The authors gratefully acknowledge the support and commitment granted by Fugro and Steve Kay.

**9. References**

Alderlieste EA and van Blaaderen EA (2015). Installation of suction caissons for an asymmetrical support structure in sandy soil. Frontiers in Offshore Geotechnics III. CRC Press 2015, Oslo, 215-220.

Andersen KH and Jostad HP and Dyvic R (2008). Penetration Resistance of Offshore Skirted Foundations and Anchors in Dense Sand. Journal of Geotechnical and Geoenvironmental Engineering. ASCE, 134(1):106-116.

ASTM (2006) D2434-68:2006. Standard test method for permeability of granular soils (Constant Head). ASTM International, West Conshohocken, PA, USA.

ASTM (2011) D2487-11:2011. Standard Practice for Classification of Soils for Engineering Purpose (Unified Soil Classification System). ASTM International, West Conshohocken, PA, USA.

Chang DS and Zhang LM (2013). Extended internal stability criteria for soils under seepage. Journal of Soils and Foundations. Elsevier, 53(4):569-583.

Chatzivasileiou IG (2014). Installation of suction caissons in layered sand, assessment of geotechnical aspects. MSc thesis, Delft University of Technology, Delft, the Netherlands.

Erbrich CT and Tjelta TI (1999). Installation of Bucket Foundations and Suction Caissons in Sand - Geotechnical Performance. Offshore Technology Conference. Houston, Texas, 725-736.

Feld T (2001). Suction Buckets: a new innovation foundation concept, applied to offshore wind turbines. PhD thesis, Aalborg University, Faculty of Engineering and Science, Department of Civil Engineering.

Fleshman MS and Rice JD (2014). Laboratory Modeling of the Mechanisms of Piping Erosion Initiation. Journal of Geotechnical and Geoenvironmental Engineering. ASCE, 140(6):04014017.

Van de Heuvel RJ and Riemers ME (2005). Self/barge Installing Platform, SIP II: the Calder experience. Frontiers in Offshore Geotechnics I. ISFOG 2005, Perth, 939-944.

Houlsby GT and Byrne BW (2005). Design procedures for installation of suction caissons in sand. Proceedings of the ICE Geotechnical Engineering. Thomas Telford, 158(3):135-144.

Houlsby GT and Kelly RB and Huxtable J and Byrne, BW (2006). Field trials of suction caissons in sand for offshore wind turbine foundations. Géotechnique. Thomas Telford, 56(1): 3-10.

Ibsen LB and Thilsted CL (2010). Numerical study of piping limits for suction installation of offshore skirted foundations and anchors in layered sand. Frontiers in Offshore Geotechnics II. CRC Press 2010, Perth, 421-426.

Panagoulias S (2015). Critical Pressure during Installation of Suction Caissons in Sand. MSc thesis, Delft University of Technology, Delft, the Netherlands.

Senders M and Randolph MF (2009). CPT-based Method for the Installation of Suction Caissons in Sand. Journal of Geotechnical and Geoenvironmental Engineering. ASCE, 135(1): 14-25.

Thielicke W and Stamhuis EJ (2014). PIVlab – Towards User-friendly, Affordable and Accurate Digital Particle Image Velocimetry in MATLAB. Journal of Open Research Software. 2(1):30.

Terzaghi K. (1943) Theoretical Soil Mechanics, John Wiley & Sons, New York, NY.

Tran MN (2005) Installation of suction caissons in dense sand and the influence of silt and cemented layers. PhD thesis, University of Sydney, 2005.

Tjelta TI (2015). The suction foundation technology. Frontiers in Offshore Geotechnics III. CRC Press 2015, Oslo, 85-93.

Villalobos FA (2007). Installation of suctions caissons in sand. Proceedings of the 6th Chilean Conference of Geotechnics (VI Congreso Chileno de Geotecnia), Valparaiso, Chile.

White DJ, Take WA and Bolton, MD (2003). Soil deformation measurement using particle image velocimetry (PIV) and photogrammetry. Géotechnique. 53(7): 619-632.